

Encapsulated Zosteric Acid Embedded in Poly[3-hydroxyalkanoate] Coatings – Protection against Biofouling

Thomas Geiger¹ (✉), Pascal Delavy², Roland Hany¹, Jürg Schleuniger¹, Manfred Zinn²

Swiss Federal Laboratories for Materials Testing and Research (EMPA): ¹Laboratory for Functional Polymers, Überlandstrasse 129, CH-8600 Dübendorf, Switzerland, ²Laboratory for Biocompatible Materials, Lerchenfeldstrasse 5, CH-9014 St. Gallen, Switzerland.
e-mail: thomas.geiger@empa.ch; Fax: +41 1 821 62 44

Received: 28 February 2004/Revised version: 13 April 2004/ Accepted: 4 May 2004

Summary

The natural, non-toxic antifouling compound zosteric acid (ZA, *p*-coumaric acid sulfate) was encapsulated in polystyrene (PS) microcapsules (30 mg ZA/1 g PS) with an efficiency of 30 % via an in-liquid drying process. Electron micrographs showed microcapsules with smooth surfaces and a mean diameter of 200 μm . The FIB method was used to cross-section a microcapsule in order to visualize the inner capsule structure and to localize ZA via element analysis. Coatings of a biocompatible polyester, poly[3-hydroxyalkanoate-*co*-3-hydroxyalkanoate] (PHAE), were prepared on microscopic slides. These coatings contained dispersed ZA (PHAE/ZA) or ZA-loaded PS microcapsules (PHAE/PS(ZA)). The release of ZA was monitored via conductivity measurements in water and was 4 $\mu\text{gcm}^{-2}\text{d}^{-1}$ for PHAE/ZA and 0.9 $\mu\text{gcm}^{-2}\text{d}^{-1}$ for PHAE/PS(ZA) coatings. To follow the initial steps of biofilm formation, coated slides were exposed to activated sludge and analyzed for cell adhesion with ESEM. ZA was effective during the burst release time of the PHAE/ZA coating, but no significant differences in biofouling were observed after 48 h. This was attributed to the minimal effective release rate of ZA, which is approximately 10 $\mu\text{gcm}^{-2}\text{d}^{-1}$.

Introduction

Marine plants are constantly exposed to harmful attacks by bacteria, spores or fungi building biofilms on the plant surfaces. In order to protect themselves some plants developed repulsion mechanisms, e.g. the seagrass *Zostera marina* L. (eelgrass). The eelgrass produces and continuously releases the water-soluble (8 % (w/w) in water) antifouling compound zosteric acid (ZA), *p*-coumaric acid sulfate. This antifoulant does not kill microorganisms but inhibits their adhesion through binding to attachment sites on cell surfaces at non-toxic concentrations [1-4].

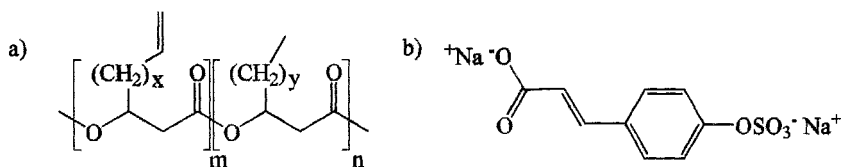
The aim of our investigation was to mimic this non-toxic protection strategy in combination with a biocompatible surface, namely a coating of poly[3-hydroxyalkanoate-*co*-3-hydroxyalkanoate], (PHAE). These polyesters have gained considerable significance in medical and industrial applications, which include

implant materials, scaffolds in tissue engineering, and packaging. ZA was blended with PHAE directly or, to control the release rate, encapsulated in polystyrene and embedded in PHAE, followed by preparation of coatings. Microcapsules have been widely used, e.g. in pharmacy for drug delivery [5]. Several techniques have been developed to produce microparticulate release systems for water-soluble drugs, including the solvent evaporation method [6-12], interfacial reaction techniques [13-16], and suspension/dispersion methods [17-19]. Here, we report on the successful encapsulation of ZA into polystyrene via the solvent evaporation method and on the characterization of these microcapsules. The preparation of PHAE coatings and release investigations are described. Finally, the adhesion of biological organisms on unprotected PHAE coatings, PHAE with dispersed ZA, and PHAE with encapsulated ZA are compared.

Experimental

Materials

Bacterial poly[3-hydroxyalkanoate-*co*-3-hydroxyalkanoate] (PHAE; Scheme 1a) with 10 % side-chain double bonds ($M_n \sim 90'000$ g/mol, $M_w \sim 210'000$ g/mol, calibration with PS-standard, $T_g = -40$ °C) was synthesized with *Pseudomonas putida* GPO1 (ATCC 29347) in chemostat cultures under multiple nutrient limited growth conditions [20, 21]. ZA was obtained from R. C. Zimmermann, Moss Landing Marine Laboratories, Moss Landing CA, USA. Polystyrene ($M_w \sim 230'000$ g/mol, $M_n \sim 140'000$ g/mol, $T_g = 94$ °C) was obtained from Aldrich and poly(vinyl alcohol) (PVA 3-98, $M_w \sim 16'000$ g/mol) from Fluka. All other reagents were used as purchased form Aldrich or Fluka.



Scheme 1: a) Poly[3-hydroxyalkanoate-*co*-3-hydroxyalkanoate] (PHAE); $m = 0.1$; $n = 0.9$; $x = 2, 4, 6$; $y = 2, 4$. b) Zosteric acid (*p*-coumaric acid sulfate).

Instruments

The particle size distribution of the microcapsules was measured with a Beckman coulter particle size analyzer LS230. The morphology examination and the elementary analysis of the microcapsules surfaces were carried out with a LEO electron microscopy 1455, equipped with an Oxford Instruments EDS system at 10 kV. Therefore, the samples were coated with a 5 nm Pt-layer using a BAL-TEC MED 020 Coating System. Cross-sections of the microcapsules were prepared by a dual beam focused ion beam (FIB) milling technique with a FEI Strata DB 235 field emission scanning electron microscope (FEG-SEM; Ga^+ -ions at 30 kV and 1000 pA). PHAE-coatings were applied with a Sogolee HP-200 air brush at 2-3 bar. Photographs of

polished cross-sections of PHAE coatings, which were fixed in epoxy resin, were taken with an Axiovert 100A (Zeiss) system. The release of ZA was monitored via conductivity by a WTW inoLab pH/Cond Level3 with a WTW TetraCon 325 probe and a MultiLab pilot program. The biofilm formation was visually analyzed with an environmental electron microscope (Amray Eco-SEM 3200 C) at 150 Torr and 20 °C.

Preparation of microcapsules and coatings

Microcapsules were prepared via an “in-liquid-drying process” in a temperature controlled reactor of 250 mL equipped with an impeller stirrer. For the oil in water (OW)-emulsion, 4 g of PS was dissolved in 16 mL methylene chloride. Subsequently, 400 mg ZA was dispersed into this solution with an Ultra Turrax (24'000 rpm, 1 min under ice cooling). This dispersion was then poured into 160 mL deionized water containing 2 % (w/w) PVA under stirring (2'000 rpm) at 20 °C for 4 h. Solid microcapsules were filtrated, washed with deionized water, and dried under reduced pressure.

Sandblasted microscope slides (area 20 cm²) were used as substrates for all coatings. PHAE coatings containing encapsulated ZA were prepared in three steps. First, a PHAE solution (1 g PHAE dissolved in 10 mL methylene chloride) was sprayed onto microscope slides with an air brush. Second, after short drying, microcapsules (about 150 mg per slide) were evenly spread on these sticky PHAE surfaces with a small brush. Finally, an additional layer of PHAE was applied to cover the microcapsules. For the preparation of PHAE coatings containing dispersed ZA, 100 mg ZA was dispersed in a PHAE solution (1 g PHAE dissolved in 10 mL methylene chloride) with an Ultra Turrax (24'000 rpm, 1 min under ice cooling). This dispersion was sprayed onto microscope slides with an air brush. After application, all coatings were dried under reduced pressure at 40 °C for 12 h.

Determination of the antifoulant content and its release

The loading of ZA in the microcapsules was determined by weighing. The loaded microcapsules were dissolved in methylene chloride, ZA was extracted with water, followed by freeze drying and weighing. The leaching of ZA from the PHAE coatings was monitored by conductivity measurements. Therefore, the coated microscope slides were stored in Millipore water (80 mL) in a completely closed glass tube. A calibrated conductivity probe recorded the release of ZA at 23 °C.

Determination of cell adhesion

The initial steps of biofilm formation (cell adhesion and attachment) were assessed in a 5 L glass beaker with pretreated, activated sludge. Test coupons were glued with silicone to the inner wall at equal heights in order to guarantee identical test conditions. Activated sludge was settled for 30 min and the supernatant was discarded. The sediment was homogenized with an Ultra Turrax at 24'000 rpm for 4 min and resuspended with a filter sterilized salt solution to the original volume. One liter of salt solution contained 85 mg KH₂PO₄, 217.5 mg K₂HPO₄, 266 mg Na₂HPO₄, 25 mg NH₄Cl, 22.5 mg MgSO₄*7H₂O, 27.5 mg CaCl₂, and 0.25 mg FeCl₃*6H₂O in demineralized water. The biomass content of the culture was determined by weight measurements and was 4.6 gL⁻¹. The test coupons were exposed to this sludge for 48

h. The coupons were sampled with a tweezers, dipped in sterile 0.9 % (w/v) NaCl, and stored in 2.5 % glutaraldehyde at 4 °C until further analysis by ESEM.

Results and discussion

Characterization of the microcapsules

This work demonstrated that the in-liquid-drying process was successful to encapsulate the hydrophilic sodium salt of ZA in a lipophilic PS matrix. Due to the high viscosity of the PS/ZA dispersion, the salt was hindered to completely dissolve in the water phase of the OW-emulsion during the microcapsule formation and hardening. The particle size measurement of the microcapsules revealed a monomodal, relatively narrow size distribution with a mean capsule diameter of 200 μm (Figure 1). The surfaces of the capsules were smooth without failures proven by SEM (Figure 2).

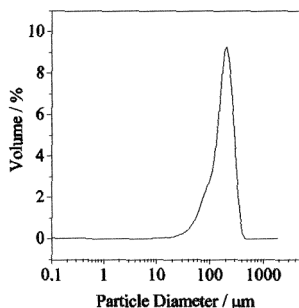


Figure 1. Particle size distribution of PS microcapsules, the mean diameter is 200 μm .

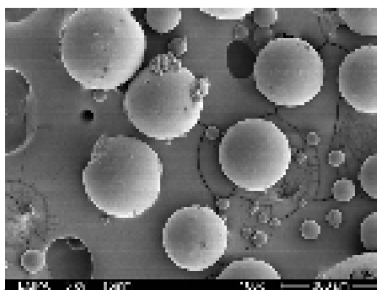


Figure 2. Electron micrograph of PS microcapsules.

The encapsulation efficiency of water-soluble compounds is generally low [5, 6]. We determined, after dissolution of the microcapsules in methylene chloride followed by water-extraction of ZA, a loading of 3 % (w/w) ZA in polystyrene capsules. This corresponds to 30 % of the maximum loading, given by the amounts of ZA (400 mg) and PS (4 g) used in the production process.

We were interested to know where ZA was localized inside the microcapsule and to visualize the inner microcapsule structure. Common methods to open microcapsules are freeze-fracture with following SEM investigations [5, 6]. We used the FIB method to cross-section a microcapsule. This method has become only recently an important tool for semiconductor device modification, as well as local micro-cross sectioning. An advantage of FIB cross-sectioning is that it can be carried out under permanent SEM control and that the Ga^+ -ion beam produces smooth cross-sections in the submicrometer range. Figure 3a shows an electron micrograph of a cross-section of a microcapsule cut by FIB. Although the PHAE/ZA dispersion was treated with ultrasound in order to remove air bubbles, the core of the PS capsule contained still empty caverns. No ZA crystals could be detected inside the microcapsule. The cross-sectioned microcapsule was therefore transferred to a SEM with EDS system for sulfur and sodium elemental analysis. The brighter areas in the electron backscatter images gave first hints of the existence of heavier elements (Figure 3b). Quantitative

element mapping with the EDS system (Figures 3c,d) clarified the position of sulfur and sodium and proved the existence of encapsulated ZA. Maps of carbon or oxygen were not conclusive, mainly due to the low ZA loading

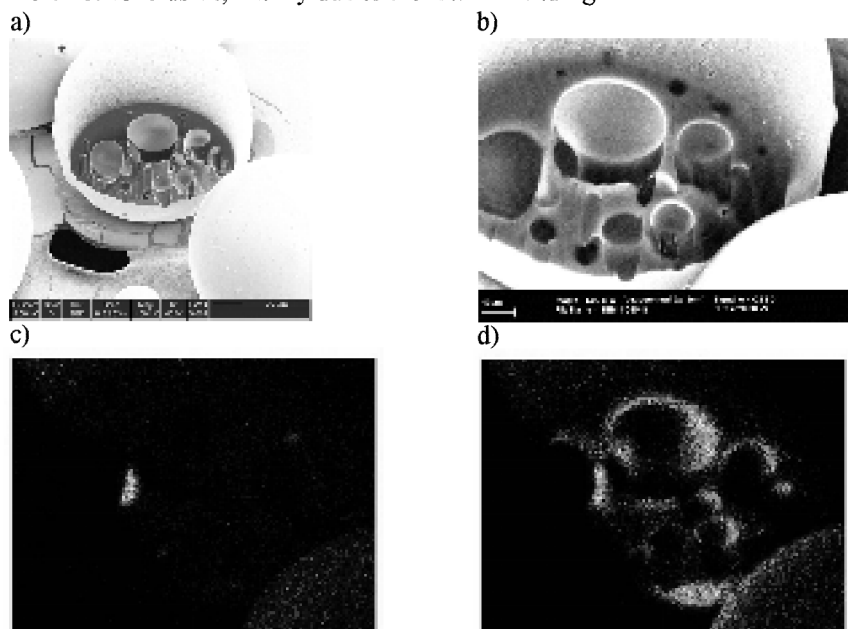


Figure 3. a) Electron micrograph of a microcapsule cross-section prepared by FIB milling, b) electron backscatter image, c) sulfur element map of the cross-section region, d) analogous sodium element map.

PHAE coatings and release

ZA encapsulated microcapsules were embedded in a PHAE coating (named PHAE/PS(ZA)). Figure 4a shows this coating applied to an objective slide (area 20 cm², approximately 4.5 mg ZA per slide), and Figure 4b its cross-section, respectively. The film thickness was about 450 μm . In contrast, the film thickness of the PHAE coating with dispersed ZA (named PHAE/ZA) was only about 50 μm (approximately 10 mg ZA per slide). Two slides of PHAE/PS(ZA) and one slide of PHAE/ZA were separately immersed in Millipore water (80 mL), and the release of ZA was monitored by changes in the water conductivity. In keeping with the biofilm formation experiments (see below), Figure 5 displays the time-course of the conductivity of both PHAE coatings for the initial 48 h. After a burst release, observable by a short increase of the conductivity during the first few hours, encapsulated ZA was released at an almost constant rate. After 48 h the release (per slide) of dispersed ZA was nearly four times than the release of encapsulated ZA. Due to the high glass transition temperature and the hydrophilicity of PS, the leaching of ZA out of the coating was hindered. On the other hand, the pure PHAE coating, which has a low glass transition temperature, had a smaller barrier effect against water. Overall, 0.9 $\mu\text{gcm}^{-2}\text{d}^{-1}$ encapsulated ZA and 4 $\mu\text{gcm}^{-2}\text{d}^{-1}$ dispersed ZA were released. This corresponds to approximately 0.8 % and 1.6 % of ZA applied. For longer

periods, the conductivities increased regularly. After 5 days, some slides showed signs of film peeling and the release measurements were finished.

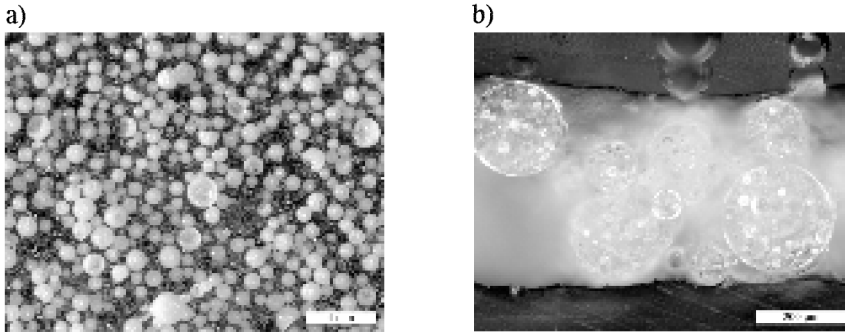


Figure 4. a) Photograph of a PHAE/PS(ZA) coating with embedded microcapsules, b) cross-section of this coating with a film thickness of about 450 μm .

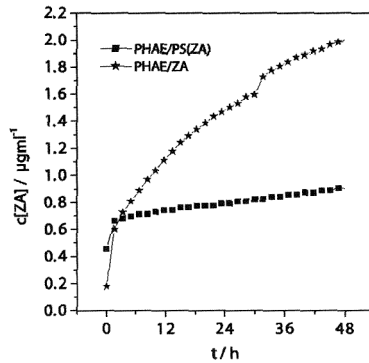


Figure 5. Release of ZA from the PHAE coatings with embedded microcapsules (PHAE/PS(ZA)) and with dispersed ZA (PHAE/ZA) monitored by changes in the water conductivity.

Biofilm formation

To examine the mode of action, biofilm formation experiments on protected and unprotected PHAE coatings were carried out. Therefore, PHAE, PHAE/PS(ZA) and PHAE/ZA coatings were exposed to diluted activated sludge in an aerated tank reactor over 48 h, a period sufficient to follow the attachment of microorganisms and the initial stages of biofilm formation [22]. Electron micrographs of original coatings and after 48 h are shown in Figure 6. Before exposure, the PHAE and PHAE/PS(ZA) coatings (Figures 6a and 6e) showed both smooth and undamaged surfaces. Small pores and elevations were visible for the PHAE/ZA coating in Figure 6c. They can be attributed to ZA crystals located near the surface; these crystals dissolved during the first three hours in contact with water and small craters were formed (Figure 6d). In contrast, the unprotected and microcapsules containing coating surfaces remained unchanged (Figures 6b, 6f). The extent of cell adhesion on the three coatings after 48 h is comparable and the unprotected PHAE surface (Figure 6b) showed not significant more bacterial settlement than the coatings containing ZA (Figure 6d, 6f). This can be

explained with the low ZA release rates determined for these coatings. The minimal effective release rate (MERR) of ZA is approximately $10 - 50 \mu\text{gcm}^{-2}\text{d}^{-1}$ [3], considerably higher than the $0.9 \mu\text{gcm}^{-2}\text{d}^{-1}$ found for the PHAE/PS(ZA) coating. Therefore, a substantial reduction in bacterial settlement should not be expected for this coating. On the other hand, the release rate for the PHAE/ZA coating was $4 \mu\text{gcm}^{-2}\text{d}^{-1}$, only slightly lower than the MEER. This agrees with the observation that during the first 2 h no cell attachment was observed on this coating. During this time of the burst release (Figure 5), the leaching rate was considerable higher and the antifouling properties of ZA became evident.

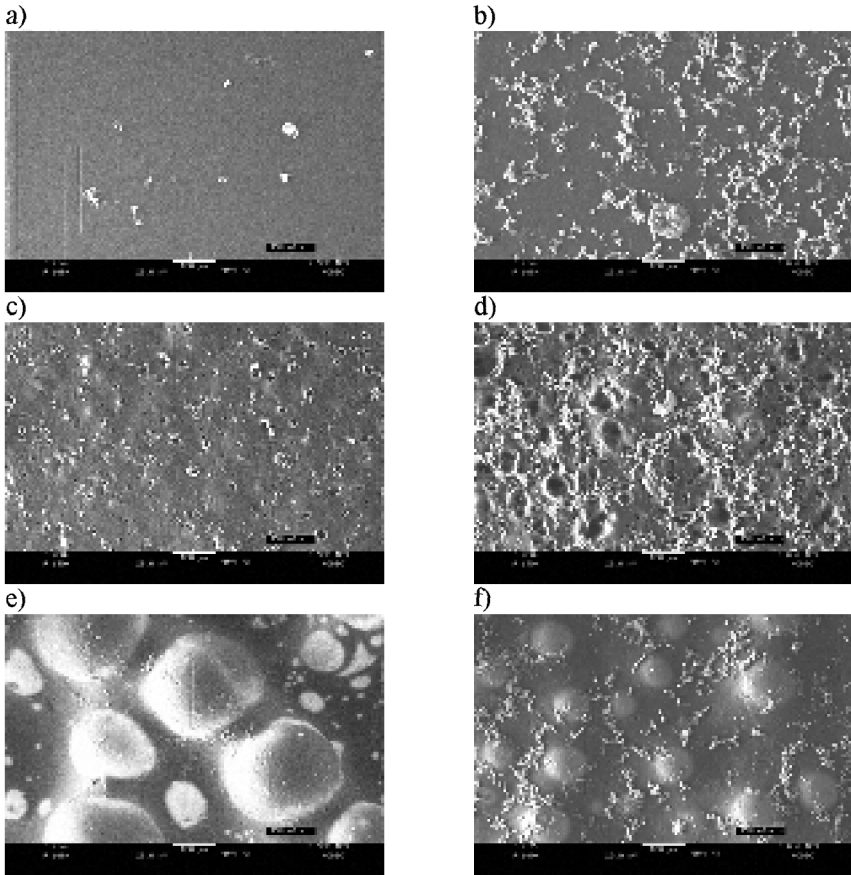


Figure 6. ESEM micrographs of original coatings and coatings after 48 h of exposure to activated sludge; a) and b) unprotected PHAE coating, c) and d) PHAE coating with dispersed ZA, e) and f) PHAE coating with encapsulated ZA; in b), d) and f) biological organisms are observable as small particles covering the coating surfaces.

Conclusion

Conventional strategies to remove a biofilm or protect a surface use highly toxic compounds that are aimed at killing the microorganisms. However, these antifoulants

are often also toxic to non-target organisms, can be accumulated through food chain amplification and cause environmental damage. This work demonstrates first results towards a more environmentally safe way to control biofouling. The flux of encapsulated ZA was lower than the minimal effective release rate. However, for ZA dispersed in PHAE, the antifouling effect was apparent during the first 2 hours of the burst release. Therefore, the encapsulation process and the loading with ZA have to be adjusted. If the size of the capsules is reduced, the increase of the capsule surface would presumably lead to a corresponding increase in the release rate. With the capsule being small enough (nanocapsules), it could even come close to the rate of the burst release of the ZA dispersion. Also, the PHAE hydrophilic-hydrophobic balance and the improvement of the coating adhesion are further steps to be optimized. Therefore, parts of the PHAE side-chain double bonds will be transformed into hydrophilic carboxyl or hydroxyl groups [23], and the remaining double bonds in the coatings cross-linked through irradiation.

Acknowledgements.

The authors thank P. Gasser for the FIB cross-sectioning, M. Trottmann for his help with the elemental analysis, and E. Pletscher for producing PHAE.

References

1. Stanley MS, Callow ME, Perry R, Alberte RS, Smith R, Callow JA (2002) *Phytopathology* 92: 378
2. Callow ME, Callow JA (1998) *Biofouling* 13: 87
3. Shin HW, Smith CM, Haslbeck EG (2001) *Journal of Environmental Biology* 22: 243
4. Todd JS, Zimmerman RC, Crews P, Alberte RS (1993) *Phytochemistry* 34: 401
5. Benita S (1996) *Microencapsulation: methods and industrial application*. Marcel Dekker, New York
6. Zydowicz N, Nzimba-Ganyanad E (2002) *Polymer Bulletin* 47: 457
7. Mandal TK, Bostanian LA, Graves RA, Chapman SR, Womack I (2002) *Drug Development and Industrial Pharmacy* 28: 339
8. Mandal TK, Bostanian LA, Graves RA, Chapman SR, Idodo TU (2001) *European Journal of Pharmaceutics and Biopharmaceutics* 52: 91
9. Schlicher E, Postma NS, Zuidema J, Talsma H, Hennink WE (1997) *International Journal of Pharmaceutics* 153: 235
10. Tabata Y, Langer R (1993) *Pharmaceutical Research* 10: 391
11. Iwata M, Nakamura Y, McGinity JW (1999) *Journal of Microencapsulation* 16: 49
12. De Rosa G, Quaglia F, Bochot A, Ungaro F, Fattal E (2003) *Biomacromolecules* 4: 529
13. Montasser I, Fessi H, Briancon S, Lieto J (2003) *Polymer Bulletin* 50: 169
14. Hirech K, Payan S, Carnelle G, Brujes L, Legrand J (2003) *Powder Technology* 130: 324
15. Yeom CK, Kim YH, Lee JM (2002) *Journal of Applied Polymer Science* 84: 1025
16. Yeom CK, Oh SB, Rhim JW, Lee JM (2000) *Journal of Applied Polymer Science* 78: 1645
17. Shukla PG, Kalidhass B, Shah A, Palaskar DV (2002) *Journal of Microencapsulation* 19: 293
18. Kriwet B, Walter E, Kissel T (1998) *Journal of Controlled Release* 56: 149
19. Okubo M, Minami H, Jing Y (2003) *Journal of Applied Polymer Science* 89: 706
20. Durner R, Zinn M, Witholt B, Egli T (2001) *Biotechnology and Bioengineering* 72: 278
21. Egli T, Zinn M (2003) *Biotechnology Advances* 22: 35
22. Zinn M, Zimmermann RC, White DC (2000) In: Evans LV (ed) *Biofilms: Recent Advances in Their Study and Control*. Harwood Academic Publishers p 361
23. Hany R, Böhlen Ch, Geiger T, Hartmann R, Kawada J, Schmid M, Marchessault RH (2004) *Macromolecules* 37: 385